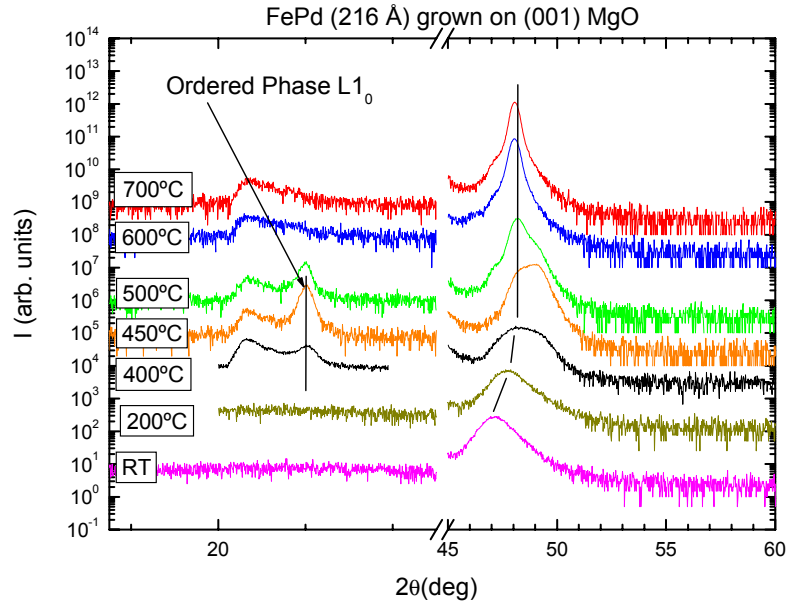


## Major Findings

### 1. FePd thin films

The structural characterization of the films grown at various substrate temperatures (RT-700°C) was performed *ex-situ* using X-Ray Diffraction (XRD). The optimum substrate temperature required to obtain long range ordered L1<sub>0</sub> FePd thin films was found by analyzing the relative intensity of various diffraction peaks in the XRD spectra (Figure 1).



**Figure 1:** XRD spectra of samples grown with the substrate held at different temperature ranging from 200°C to 700°C.

The growth rate was calibrated from XRD studies at low angle on one of the samples (RT, 15 min growth) and found to be 14.4 Angstroms/min (Figure 2).

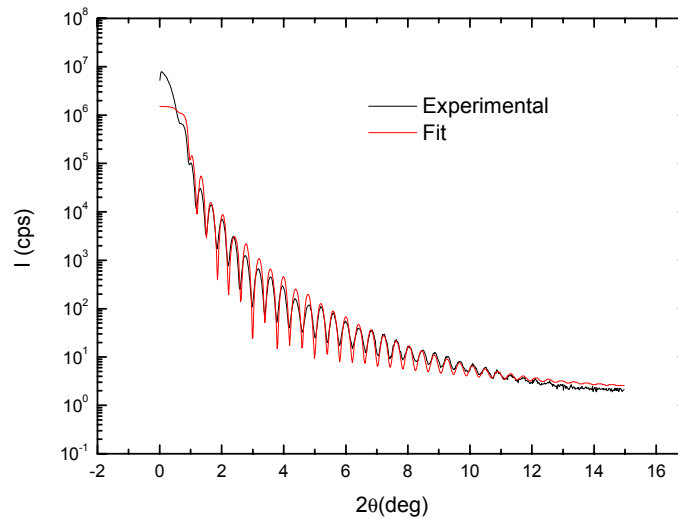


**Figure 2.** Low angle XRD for FePd film grown at RT.

The magnetic properties of the samples were characterized using longitudinal and polar magneto-optical Kerr effect. (Figure 3)

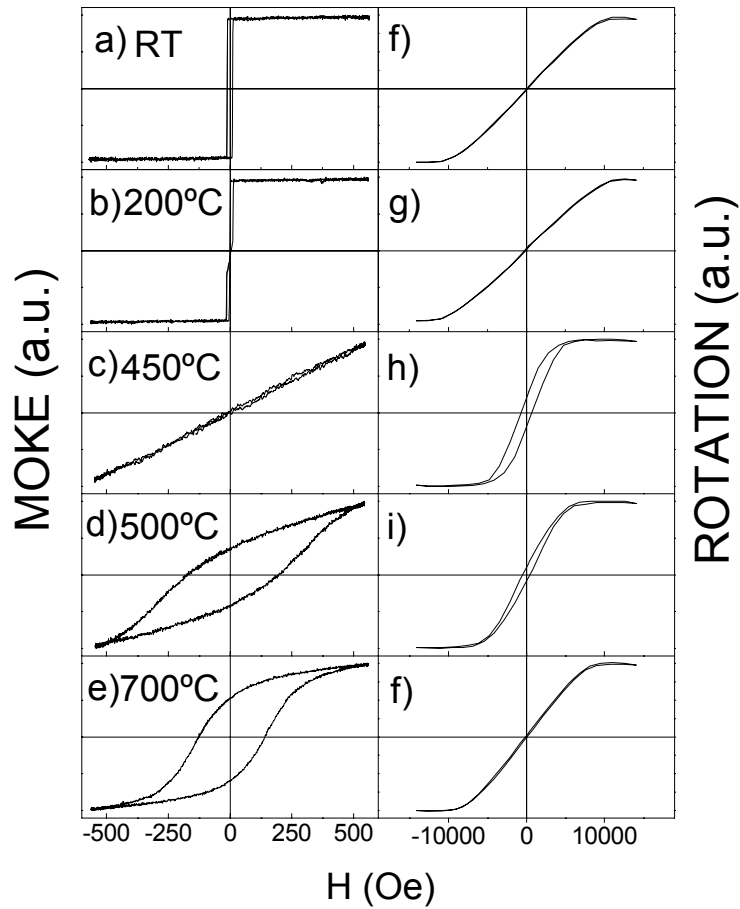


**Figure 3.** Hysteresis loops measured with longitudinal Kerr geometry (left column) and polar Kerr geometry (right column) for FePd samples ( $\sim 21$  nm thick).

The above data can be summarized in the following table:

Growth temperature	Growth mode	Film structure
RT-200°C	2D growth	Mostly disordered
400°C-450°C	2D growth	Long range order
500°C	3D growth	Order + disorder
600°C-700°C	3 D growth	Mostly disordered

Thus, the correlation between XRD and MOKE established that the optimum substrate temperature for films with significant long range L1o order and perpendicular magnetic anisotropy was 450°C.

A series of samples of varying thickness were grown at 450°C and later characterized with *ex-situ* XRD, AFM/MFM and MOKE. A set of samples was not capped while to other sets were capped with 20 Angstroms of Pd and 30 Angstroms MgO respectively. From the integrated diffraction-peak intensities of several peaks [e.g. (100) and (200)] the degree of long-range order was estimated to be very similar in all the samples. Detailed cross-sectional TEM studies are currently in progress to correlate with the XRD data. (Figure 4).

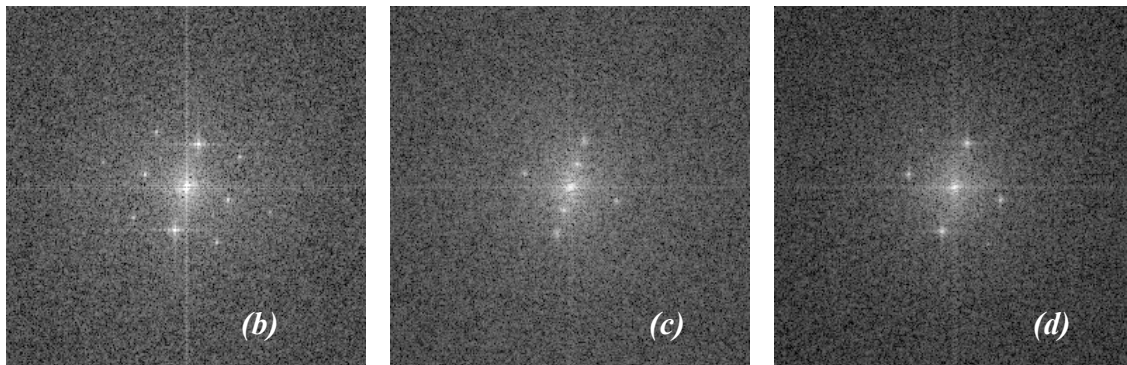
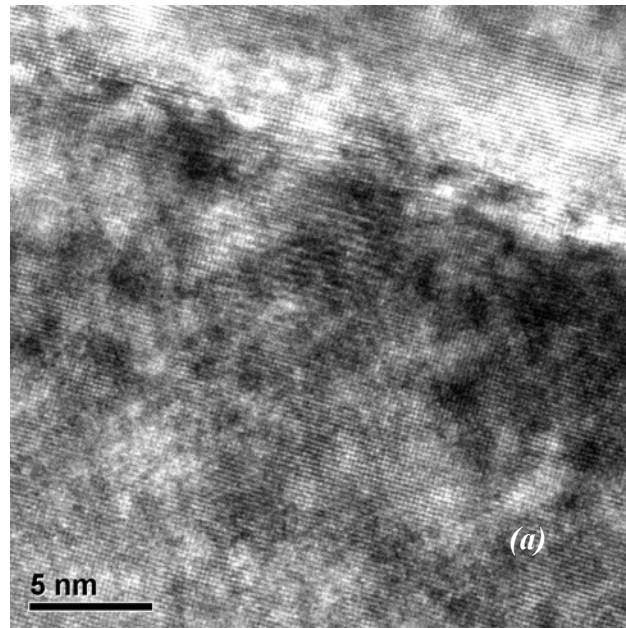


**Figure 4.** (a) HRTEM image showing the MgO substrate (top) and the FePd film (bottom). We notice that the film has crystalline structure following the epitaxy on the MgO substrate and that there are regions in the film that exhibit a periodic structure parallel to the film/substrate interface that has twice the period of other regions, indicating high chemical order with L1o structure. FFT transforms of various regions confirm this. (b) FFT corresponding to the substrate; (c) FFT corresponding to the highly ordered region. We observe only one direction where there are intermediate spots in the four-fold symmetric pattern, corresponding with the fringes parallel to the interface; (d) FFT corresponding to a crystalline but chemically disordered region in the film.

The magnetic characterization of these samples was done using polar MOKE. Thus, hysteresis cycles as well as the spectral dependence of  $\theta_K$  were determined. (Figures 5,6)

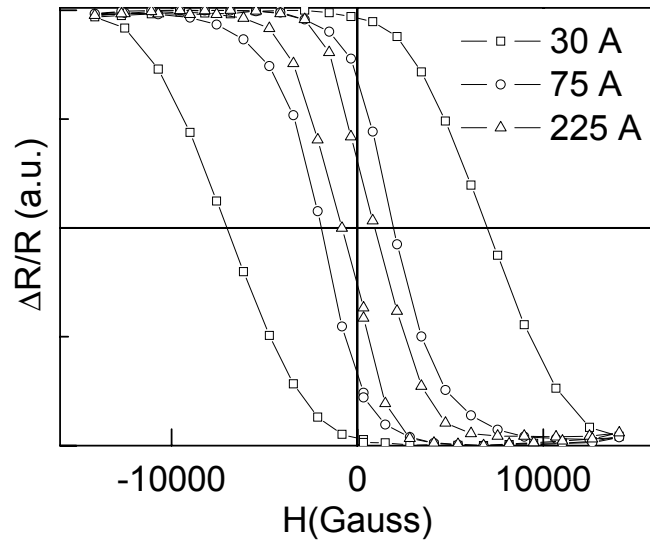


**Figure 5.** Hysteresis loops in polar Kerr geometry for a series of MgO-capped FePd samples of thickness 30, 75 and 225 Angstroms respectively.

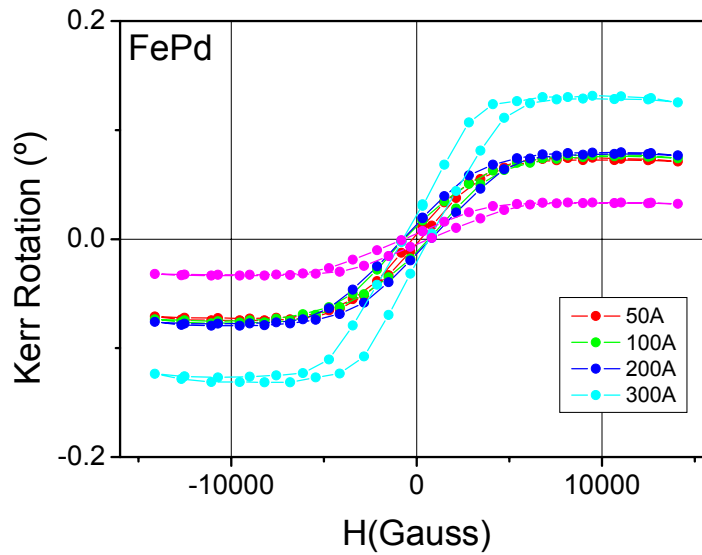


**Figure 6.** Hysteresis loops in polar Kerr geometry measured for a series of epitaxial FePd films (50-300 Angstroms thick) grown at 450°C on (001) MgO and capped with 20 Angstroms Pd.

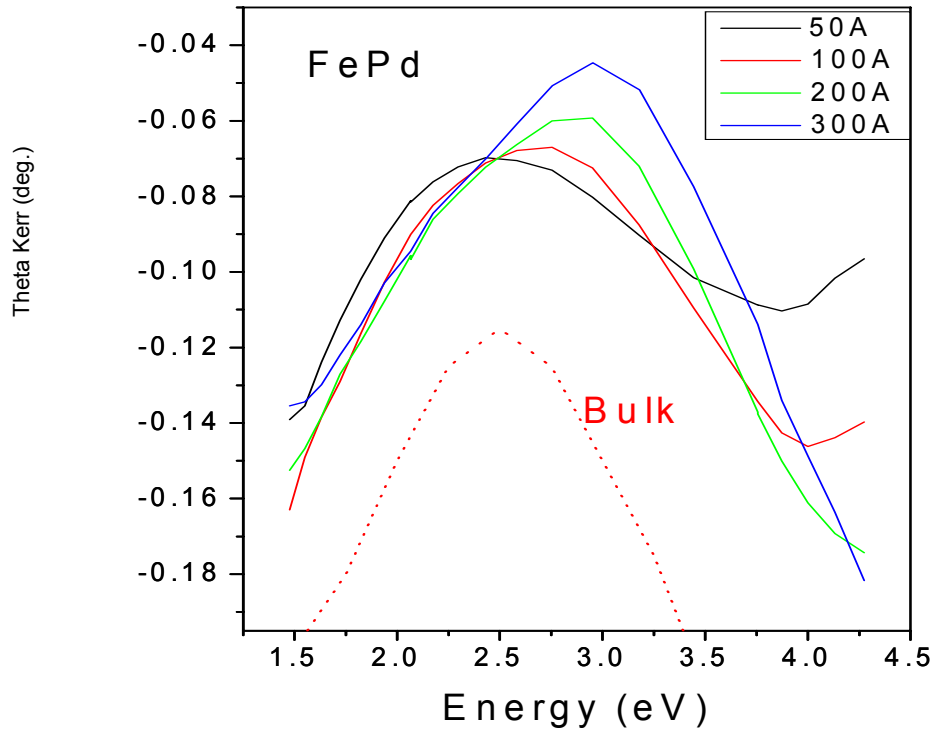


**Figure 7.** Spectral dependence of  $\theta_K$  for FePd highly ordered films (Pd-capped) and bulk  $\text{Fe}_{0.5}\text{Pd}_{0.5}$  for comparison.

The experimental spectra obtained for the samples were compared to published spectra for bulk  $\text{Fe}_{0.5}\text{Pd}_{0.5}$ . We notice that the thinner films exhibit maxima at similar energy than bulk while the thicker films have maxima shifted towards higher energies. We are currently analyzing these data.

Regarding the hysteresis loops, we notice that there is different trend depending on the capping of the samples. The MgO-capped samples exhibit larger coercive fields scaling in inverse relation with film thickness, while the coercive fields observed for the Pd-capped samples are smaller but scale in direct proportion with film thickness. We also observed with longitudinal MOKE that the magnetization exhibits a component parallel to the surface of the films, and therefore the magnetization vector at the surface of the films is canted. We postulate that the Pd in the capping layer may be polarized in the latter set, facilitating closure domains with magnetization component parallel to the film surface. This was not the case for MgO capped films, where we could not saturate the films in the direction parallel to the plane of the films for fields as large as 1.2 Tesla. We postulate that in this case the oxide capping layer does not facilitate closure domains at the surface and therefore highly anisotropic nano-regions in the film are harder to reverse and hence the larger coercivity. Modeling of the data to address this trends is in progress.

The surface morphology of the films was studied with *ex-situ* AFM. (Figure 8, 9)

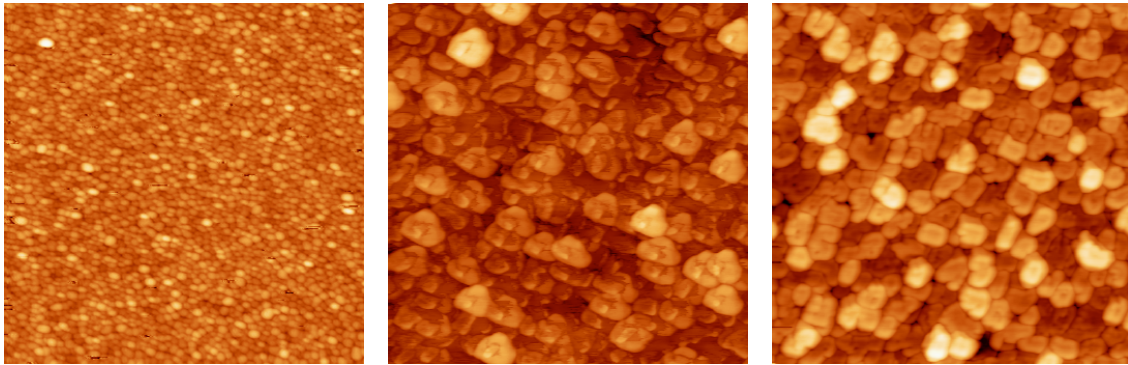


**Figure 8.** Surface morphology of non-capped FePd films of thickness 30, 75 and 225 Angstroms respectively.

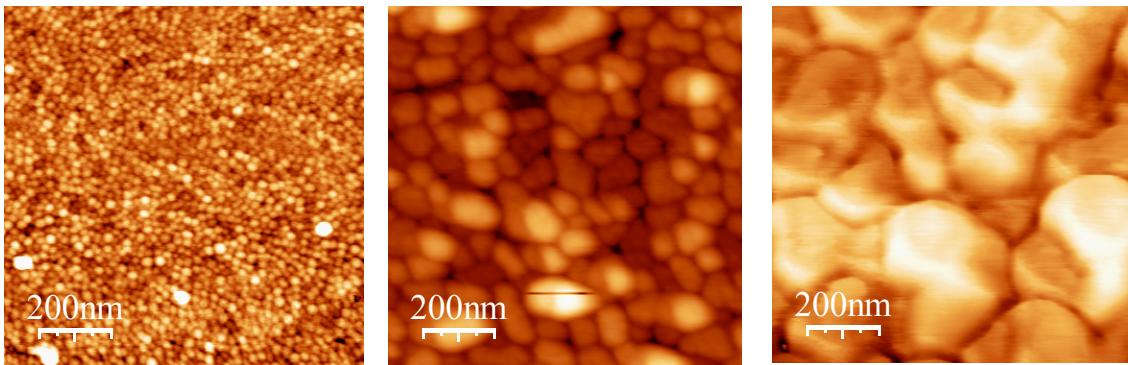


**Figure 9.** Surface morphology of capped FePd films of thickness 50, 100 and 250 Angstroms respectively.

We notice the typical “island” size and inter-island distance scales with the thickness of the films, regardless of the capping material used, thus studies regarding scaling properties of the surface features are in progress. We also notice that capped films tend to be smoother than non-capped ones.

An important aspect of our studies is to try also to find correlation between surface features and magnetic properties. Thus, correlated magnetic force microscopy images were obtained on the same regions of the samples where the topographic images discussed above were obtained. The domain size was measured to perform correlated studies between domain-size, surface morphology and microstructure of the samples. (Figure 10).

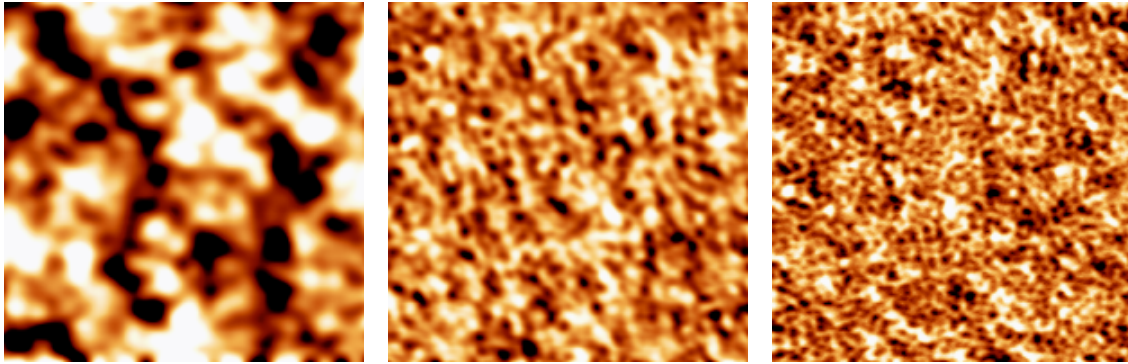


**Figure 10.** Magnetic force imaging of capped FePd films of thickness 50, 100 and 250 Angstroms respectively.

Domain-size measurements were estimated from the MFM images using two methods: FFT analysis and a graphic method (from Hubert and Schafer, “Magnetic Domains”, Springer, 2000). The measurements are summarized in the following table:

sample	image	D_FFT (nm)	D_ster (nm)
120504A 25 nm thick	2	150	
	4		120
	reman4	150	
	reman3		140
130504A 20 nm thick	11	180	
	12		140
	reman3	170	
	reman4		130
120504B 10 nm thick	22	390	
	23		260
	reman4	290	
	reman2		160
130504B 5 nm thick	13	550	
	12		790
	reman1	590	
	13		130

We notice inverse scaling of the domain size with increasing film thickness. These results are currently being analyzed and correlated with the additional information obtained on the microstructure and surface morphology of the samples. Modeling of the data is in progress.

## 2. FePt thin films

The conditions for the growth of epitaxial FePt thin films with long range order were investigated using *ex-situ* XRD (Figure 11).

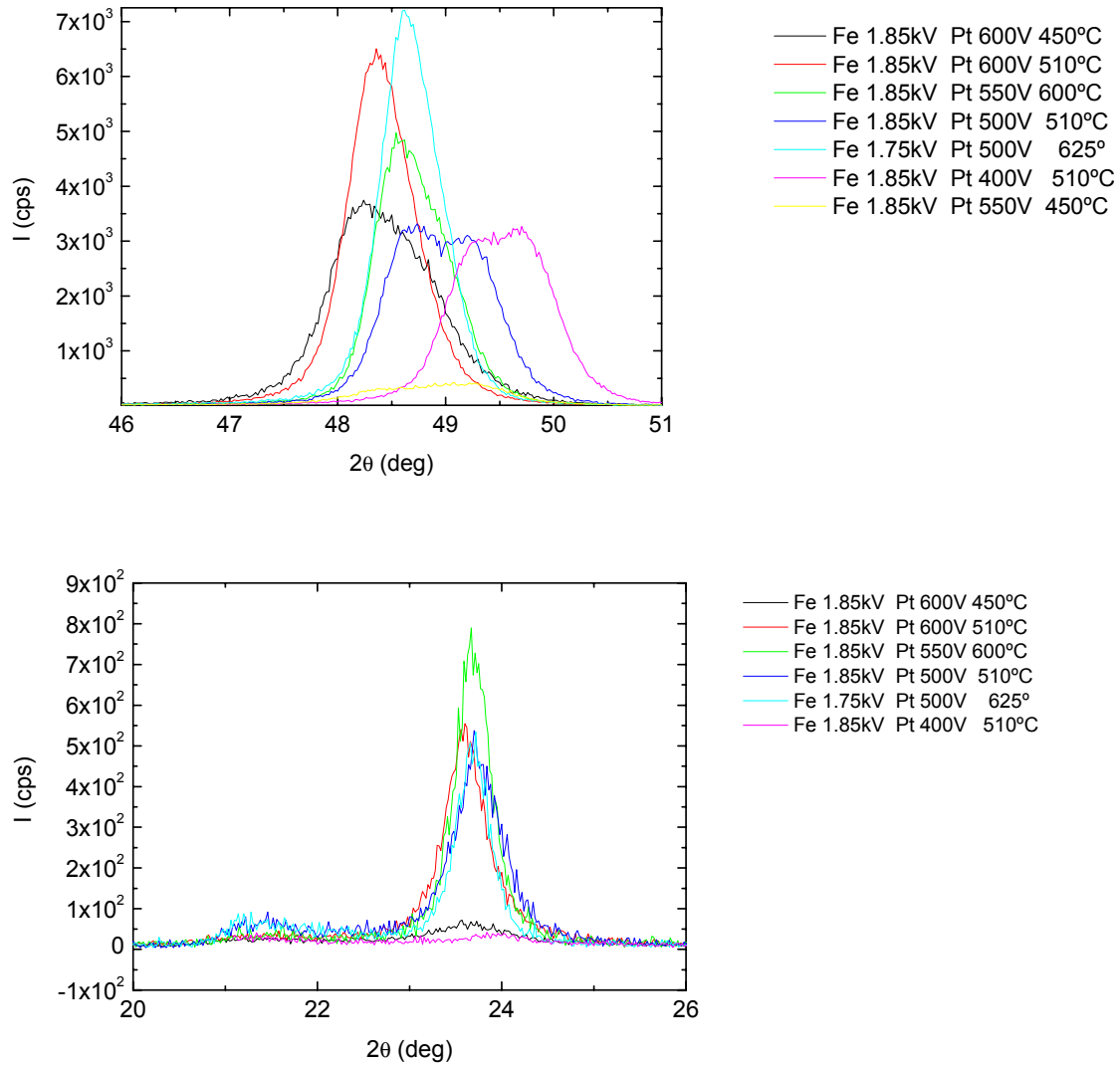


**Figure 11.** XRD spectra for FePt films grown on (001) MgO.

The microstructure of the films is currently being investigated with *ex-situ* cross sectional TEM. (Figure 12)



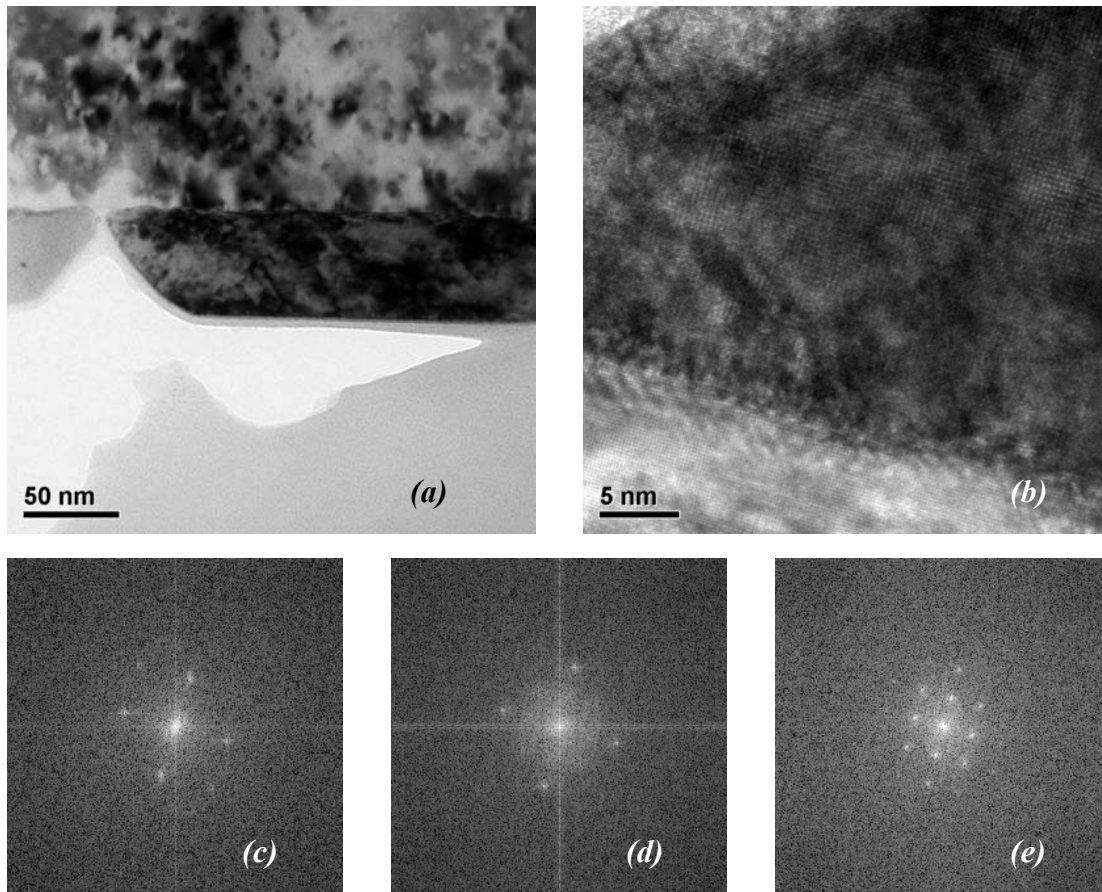


**Figure 12.** (a) Cross sectional TEM image of an epitaxial FePt sample; (b) atomic resolution TEM image showing nano-regions with high chemical order (L1o); (c) FFT transform of the region in the HRTEM image that corresponds to the substrate; (d) FFT transform of the region in the same image that corresponds to the crystalline but chemically disordered FePt thin film; (e) FFT transform of the region in the image corresponding to the highly ordered region. We notice that there are intermediate spots in the four-fold symmetric pattern in both orthogonal directions.

The preliminary TEM data seems to indicate that FePt has much better epitaxy than the FePd films (no tilting or micro domains) and the grains are single domain L1o ordered.

The magnetic properties of these films were investigated with Kerr magnetometry in the polar configuration. (Figure 13). We notice that despite the fact that we have obtained films with nano-regions with high chemical order (L1o), the anisotropy still favors in-plane magnetization. Further studies on these films are in progress.

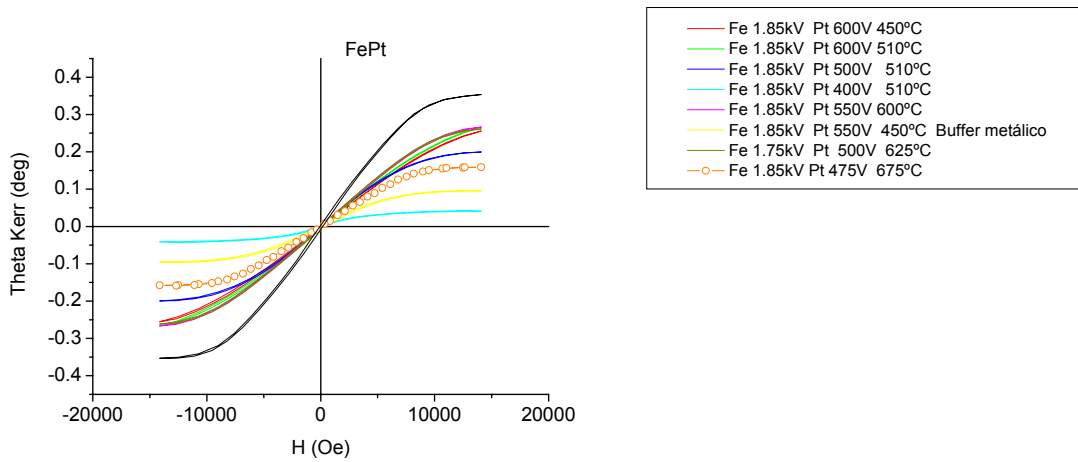


**Figure 13.** Polar Kerr magnetometry of epitaxial FePt films.

### 3. Ion-implantation to achieve highly anisotropic shallow nano-clusters

A preliminary sample was prepared using ion implantation at THIA (Toledo Heavy Ion accelerator). The conditions for the ion-implantation were chosen to achieve a shallow (i.e. approximately topmost 50 Angstroms) deposition of Fe nano-clusters. The preliminary sample was (001) Si that was implanted with iron ions at an incident ion energy of 30 keV and a dose of  $2.5 \times 10^{16}$  /cm<sup>2</sup>. The sample was kept at room temperature during implantation. Afterwards, the sample was characterized with MOKE. A noisy and weak magnetic signal was observed. (Figure 14).

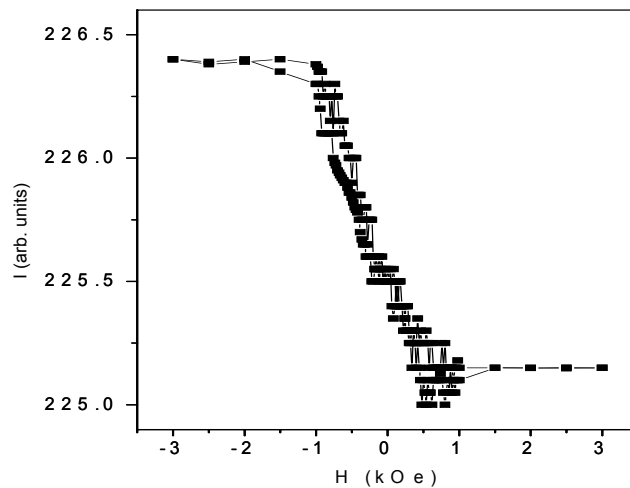


**Figure 14.** Longitudinal Kerr magnetometry of Si ion-implanted sample.

We have applied the ion implantation process to epitaxial Pt films grown on (001) MgO. Thus, a Pt thin film sample, epitaxially grown on (001) MgO was implanted under similar conditions than the Si sample but the planned dose is  $5.0 \times 10^{16} / \text{cm}^2$  in order to enhance the magneto-optical signal. After ion implantation, the sample was annealed at  $450^\circ\text{C}$  for one hour. Correlated studies between structure and magnetic properties are currently in progress. Figure 15 shows polar Kerr hysteresis loops for the implanted sample before and after annealing.

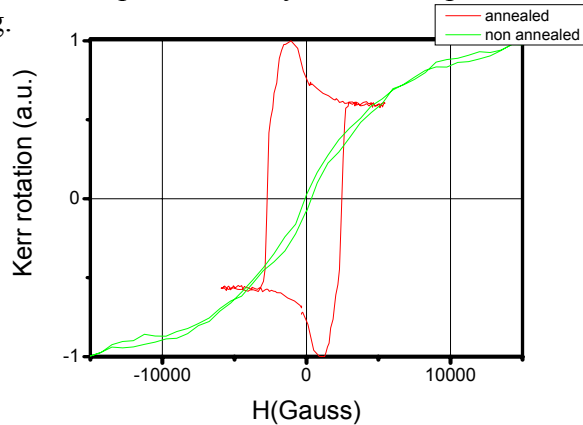


**Figure 15.** Polar Kerr hysteresis loops for ion-implanted Pt film.

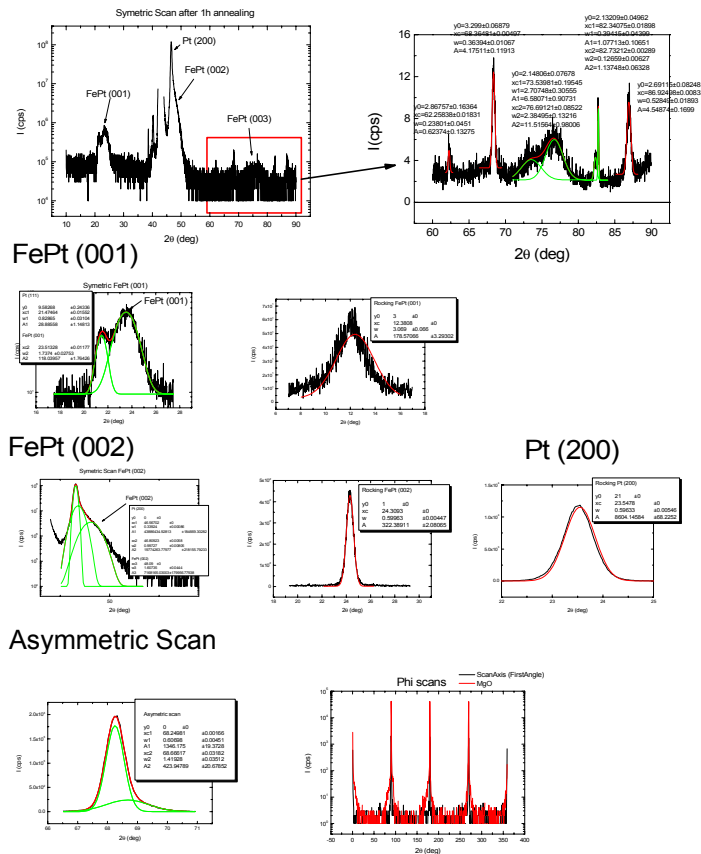


**Figure 16.** XRD charts showing the formation of the highly ordered L10 phase.

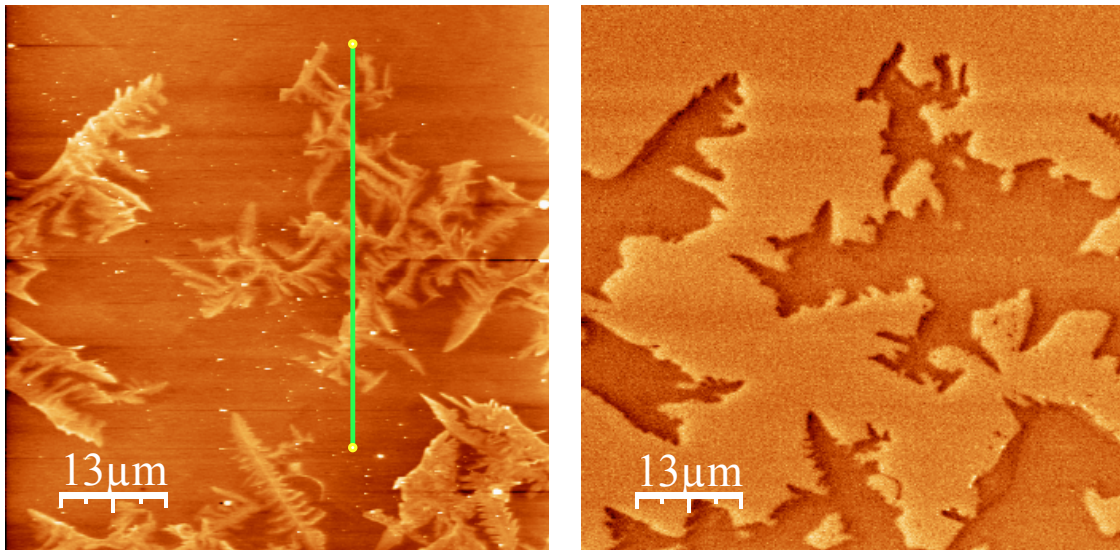


**Figure 17.** Left: Topographic AFM and right: MFM image of the Fe implanted Pt thin film sample after UHV annealing.

Structural characterization (Figure 16) as well as surface morphology measurements (Figure 17) indicate that the Fe implanted Pt thin film sample has formed small L1<sub>0</sub> clusters near the surface with perpendicular magnetization.

Further studies are in progress to determine the effect of rapid thermal annealing (RTA) on ion-implanted samples, to obtain smaller clusters.